TABLE III – 41 BAC CLONES WHICH COULD DISCRIMINATE HCCS IN POOR-OUTCOME GROUP (P) FROM THOSE IN FAVORABLE-OUTCOME GROUP (F)

BAC clone ID	Location	Cutoff value	DNA methylation status[1]	Sensitivity (%)	Specificity (%)
RP11-89K16	1p35	1.50	F<P	83.3	100.0
RP11-201O14	1p34.3-1p36.13	1.22	F>P	100.0	100.0
RP11-156K6	1p31.1-1p31.3	1.15	F>P	100.0	80.0
RP11-553K8	1q31.2-1q31.3	1.16	F>P	100.0	100.0
RP11-89E10	1q31.3	0.91	F<P	100.0	100.0
RP11-180L21	2p16-2p21	1.29	F>P	100.0	80.0
RP11-90B13	2p14-2p15	1.13	F>P	83.3	100.0
RP11-449B19	2q11.2	0.75	F<P	100.0	80.0
RP11-30M1	2q32.3	1.10	F<P	100.0	100.0
RP11-89B13	2q32.3-2q33.1	1.11	F>P	83.3	80.0
RP11-255O19	3p24.3-3p25	1.08	F>P	100.0	100.0
RP11-421F9	3p24.2a	0.97	F>P	83.3	100.0
RP11-122D19	3p21.2	0.99	F<P	100.0	80.0
RP11-36K8	4q22	0.91	F>P	83.3	100.0
RP11-101N17	4q26	0.85	F<P	100.0	100.0
RP11-177L7	4q32	0.94	F>P	100.0	100.0
RP11-13O14	4q34-4q35	0.88	F<P	83.3	100.0
RP11-88H16	5p14	0.85	F<P	100.0	100.0
RP11-91G9	5q22-5q23	1.45	F<P	83.3	100.0
RP11-79K22	6q16	0.98	F<P	83.3	100.0
RP11-126B8	7q21.3	1.06	F>P	100.0	100.0
RP11-89P11	7q35	0.83	F>P	83.3	100.0
RP11-88N8	8q21.11d	1.02	F>P	100.0	100.0
RP11-85C21	9q33.3-9q34.2	0.95	F<P	83.3	100.0
RP11-714M16	10q26.11-10q26.3	1.00	F<P	100.0	100.0
RP11-48A2	10q26.2	0.69	F<P	100.0'	80.0
RP11-206I1	11p11.2	1.20	F<P	100.0	100.0
RP11-35F11	11q12	1.30	F<P	100.0	80.0
RP11-158I9	11q23	1.04	F>P	83.3	100.0
RP11-74I8	12q13	1.13	F<P	100.0	100.0
RP11-167B4	16p13.3	0.97	F>P	83.3	100.0
RP11-368N21	16p11.2-16p12	1.10	F>P	83.3	100.0
RP11-303G21	16q12.1b	0.80	F>P	83.3	100.0
RP11-151M19	16q22	1.05	F>P	100.0	100.0
RP11-135N5	17p13.2	1.00	F>P	100.0	100.0
RP11-398A1	17q11.2d	1.00	F>P	100.0	100.0
RP11-15A1	19q13	1.08	F>P	83.3	100.0
RP11-697B10	19q13.3	0.90	F>P	83.3	100.0
RP11-79A3	19q13.3	1.05	F<P	100.0	100.0
RP11-29H19	20q12	1.00	F>P	100.0	100.0
RP11-36N5	22q11.2	1.15	F>P	83.3	100.0

[1]F>P, when the signal ratio was lower than the cutoff value, the tissue sample was considered to have been obtained from a patient with poor prognosis; F<P, when the signal ratio was higher than the cutoff value, the tissue sample was considered to have been obtained from a patient with poor prognosis.

identifying reproducible indicators for carcinogenetic risk estimation and prognostication. In fact, we have successfully obtained optimal indicators for carcinogenetic risk estimation and prognostication of renal cell carcinomas[26] and urothelial carcinomas (data will be published elsewhere) by BAMCA using the same array as that used in this study.

Our previous studies indicated that alterations of DNA methylation are one of the earliest events of multistage hepatocarcinogenesis and participate in malignant progression of HCCs.[5,7-14,27-29] However, since in previous studies we examined DNA methylation status on only a restricted number of CpG islands or chromosomal loci, it has not yet been clarified whether DNA methylation status on only restricted regions is simply altered at the precancerous stage, or whether genome-wide alterations of DNA methylation status have certain clinicopathological significance. As shown in Panel N of Figure 1*b*, genome-wide DNA methylation alterations (both hypo- and hypermethylation) were confirmed even in noncancerous liver tissue samples obtained from patients with HCCs. The number of BAC clones showing DNA methylation alterations and the degree of DNA methylation alterations were found to increase stepwise from the precancerous stage to the HCC stage (Fig. 1*b* and Table I). This study revealed that alterations of DNA methylation during multistage hepatocarcinogenesis occur in a genome-wide manner. Genome-wide DNA methylation alterations may participate in multistage hepatocarcinogenesis potentially through the induction of chromosomal instability and silencing of tumor-suppressor genes. DNA methylation alterations in noncancerous liver tissue were correlated with the future development of HCCs, suggesting that DNA methylation alterations at the precancerous stage may not occur randomly but are prone to further accumulation of genetic and epigenetic alterations.

Although mass vaccination against HBV has been initiated, this will not have a major impact for many years, as the age at presentation of HBV is older than 50 years mainly in Asia and Africa.[30] The spread of HCV in Japan that occurred in the 1950s and 1960s has resulted in a rapid increase in the incidence of HCC since 1980. In other countries including the United States, where HCV infection spread more recently, an increase in the incidence of HCC is imminent.[31] Although there were no significant differences in the number of BAC clones showing DNA hypo- or hypermethylation between HBV- and HCV-positive patients with HCCs, Wilcoxon test identified BAC clones in which DNA methylation status differed significantly between HBV- and HCV-positive patients with HCCs in both noncancerous liver tissue and cancerous tissue, suggesting that the HBV-related carcinogenetic

TABLE IV – MULTIVARIATE ANALYSIS OF CLINICOPATHOLOGICAL PARAMETERS AND DNA METHYLATION PROFILES ASSOCIATED WITH OVERALL OUTCOME IN PATIENTS WITH HCCS

Parameters	Hazard ratio (95% CI)	χ^2	p
Histological differentiation			
Well differentiated	1 (Reference)	0.031	0.8594
Moderately or poorly differentiated	0.817 (0.088-7.616)		
Portal vein tumor thrombi			
Negative	1 (Reference)	2.095	0.1478
Positive	4.474 (0.588-34.033)		
Intrahepatic metastasis[1]			
Negative	1 (Reference)	0.090	0.7647
Positive	1.248 (0.292-5.336)		
Multicentricity[1]			
Negative	1 (Reference)	1.499	0.2209
Positive	0.328 (0.055-1.955)		
The criteria of Table 3			
Satisfying for less than 32 BAC clones	1 (Reference)	4.997	0.0254
Satisfying for 32 or more BAC clones	4.466 (1.202-16.585)		

CI, confidence interval.
[1]In patients with multiple lesions, whether the lesions other than the main tumor from which tissue samples were obtained for this study were intrahepatic metastases of the main tumor or second primary lesions was judged by microscopic observation of hepatectomy specimens based on the previously described criteria.[35]

pathway may result in distinct DNA methylation profiles. These findings are in accordance with a previous report showing that HBV-related proteins can induce DNA methylation alterations.[32]

The effectiveness of surgical resection for HCC is limited, unless the disease is diagnosed early at the asymptomatic stage. Therefore, surveillance at the precancerous stage will become a priority. To reveal the baseline liver histology, microscopic examination of liver biopsy specimens is performed in patients with HBV or HCV infection prior to interferon therapy.[33,34] Therefore, carcinogenetic risk estimation using such liver biopsy specimens will be advantageous for close follow-up of patients who are at high risk of HCC development. Because even subtle alterations of DNA methylation profiles at the precancerous stage are stably preserved on DNA double strands by covalent bonds, they may be better indicators for risk estimation than mRNA and protein expression profiles that can be easily affected by the microenvironment of precursor cells.

The present genome-wide analysis revealed DNA methylation profiles that were able to discriminate noncancerous liver tissue obtained from patients with HCCs from normal liver tissue and diagnose it at high risk of HCC development in the learning set. The sensitivity and specificity in the validation set were 95.8 and 96.2%, respectively, and the criteria listed in Table II were validated. For carcinogenetic risk estimation using liver biopsy specimens obtained prior to interferon therapy, DNA methylation profiles actually associated with carcinogenesis should be discriminated from those associated with inflammation and/or fibrosis. Therefore, we first omitted potentially insignificant BAC clones associated only with inflammation and/or fibrosis and focused on BAC clones for which DNA methylation status was inherited by HCCs from the precancerous stage (Groups I, II, III and IV). In fact, it was confirmed that there were no significant differences in the number of BAC clones satisfying the criteria in Table II between noncancerous liver tissue samples showing chronic hepatitis and noncancerous liver tissue samples showing cirrhosis, not only in the learning set ($p = 0.542$) but also in the validation set ($p = 0.128$), indicating that our criteria were not associated with the degree of inflammation or fibrosis. In addition, the average numbers of BAC clones satisfying the criteria in Table II were significantly lower in liver tissue of patients without HCCs (V1 to V7) than in noncancerous liver tissue of patients with HCCs (N1 to N39), even though the patients from whom V1 to V7 were obtained were infected with HBV or HCV. Therefore, our criteria not only discriminate noncancerous liver tissue obtained from patients with HCCs from normal liver tissue but may also be applicable for classifying liver tissue obtained from patients who are followed up because of HBV or HCV infection, chronic hepatitis or cirrhosis into that which may generate HCCs and that which will not. Our criteria are applicable to both patients with chronic hepatitis and liver cirrhosis, although liver cirrhosis is known to show a more pronounced tendency to lead to HCC development than chronic hepatitis.[20] We intend to validate the reliability of such risk estimation prospectively using liver biopsy specimens obtained prior to interferon therapy from a large cohort of patients. On the basis of the present data, we now consider it justifiable to propose that clinicians can apply a portion of biopsy cores for this type of prospective study.

Because a sufficient quantity of good-quality DNA can be obtained from liver biopsy specimens, PCR-based analyses focusing on individual CpG sites are not always required. Although cut-off values should be modified for widely available standardized reference DNA, array-based analysis that overviews aberrant DNA methylation in each BAC region is immediately applicable to routine laboratory examinations. Moreover, because DNA methylation status of CpG sites is often regulated in a coordinated manner in each individual large region on chromosomes,[13,14,25] an overview of the DNA methylation tendency (hypo- or hypermethylation) in the whole BAC region can be a more reproducible diagnostic indicator than one focusing on individual CpG sites.

The present genome-wide analysis revealed DNA methylation profiles that were able to discriminate a poor-outcome group from a favorable-outcome group. Correlation between the DNA methylation profiles and both cancer-free and overall survival rates of patients with HCCs (Fig. 3*d*) validated the criteria in Table III. Prognostication based on our criteria may be promising for supportive use during follow-up after surgical resection, because multivariate analysis revealed that our criteria can predict overall patient outcome independently of parameters observed in hepatectomy specimens that are already known to have prognostic impact.[20] Such prognostication using liver biopsy specimens obtained before transarterial embolization, transarterial chemoembolization and radiofrequency ablation may be advantageous even to patients who undergo such therapies. The reliability of such prognostication needs to be validated again prospectively in surgically resected specimens or biopsy specimens.

References

1. Jones PA, Baylin SB. The fundamental role of epigenetic events in cancer. Nat Rev Genet 2002;3:415–28.
2. Gronbaek K, Hother C, Jones PA. Epigenetic changes in cancer. APMIS 2007;115:1039–59.
3. Eden A, Gaudet F, Waghmare A, Jaenisch R. Chromosomal instability and tumors promoted by DNA hypomethylation. Science 2003; 300:455.
4. Baylin SB, Ohm JE. Epigenetic gene silencing in cancer—a mechanism for early oncogenic pathway addiction? Nat Rev Cancer 2006;6:107–16.
5. Kanai Y, Ushijima S, Tsuda H, Sakamoto M, Sugimura T, Hirohashi S. Aberrant DNA methylation on chromosome 16 is an early event in hepatocarcinogenesis. Jpn J Cancer Res 1996;87: 1210–7.
6. Yoshiura K, Kanai Y, Ochiai A, Shimoyama Y, Sugimura T, Hirohashi S. Silencing of the E-cadherin invasion-suppressor gene by CpG methylation in human carcinomas. Proc Natl Acad Sci USA 1995;92:7416–9.
7. Kanai Y, Ushijima S, Hui AM, Ochiai A, Tsuda H, Sakamoto M, Hirohashi S. The E-cadherin gene is silenced by CpG methylation in human hepatocellular carcinomas. Int J Cancer 1997; 71:355–9.
8. Kanai Y, Hui AM, Sun L, Ushijima S, Sakamoto M, Tsuda H, Hirohashi S. DNA hypermethylation at the D17S5 locus and reduced HIC-1

mRNA expression are associated with hepatocarcinogenesis. Hepatology 1999;29:703–9.
9. Sun L, Hui AM, Kanai Y, Sakamoto M, Hirohashi S. Increased DNA methyltransferase expression is associated with an early stage of human hepatocarcinogenesis. Jpn J Cancer Res 1997;88:1165–70.
10. Saito Y, Kanai Y, Sakamoto M, Saito H, Ishii H, Hirohashi S. Expression of mRNA for DNA methyltransferases and methyl-CpG-binding proteins and DNA methylation status on CpG islands and pericentromeric satellite regions during human hepatocarcinogenesis. Hepatology 2001;33:561–8.
11. Saito Y, Kanai Y, Nakagawa T, Sakamoto M, Saito H, Ishii H, Hirohashi S. Increased protein expression of DNA methyltransferase (DNMT) 1 is significantly correlated with the malignant potential and poor prognosis of human hepatocellular carcinomas. Int J Cancer 2003;105:527–32.
12. Saito Y, Kanai Y, Sakamoto M, Saito H, Ishii H, Hirohashi S. Overexpression of a splice variant of DNA methyltransferase 3b. DNMT3b4, associated with DNA hypomethylation on pericentromeric satellite regions during human hepatocarcinogenesis. Proc Natl Acad Sci USA 2002;99:10060–5.
13. Kanai Y, Hirohashi S. Alterations of DNA methylation associated with abnormalities of DNA methyltransferases in human cancers during transition from a precancerous to a malignant state. Carcinogenesis 2007;28:2434–42.
14. Kanai Y. Alterations of DNA methylation and clinicopathological diversity of human cancers. Pathol Int 2008;58:544–58.
15. Gao W, Kondo Y, Shen L, Shimizu Y, Sano T, Yamao K, Natsume A, Goto Y, Ito M, Murakami H, Osada H, Zhang J, et al. Variable DNA methylation patterns associated with progression of disease in hepatocellular carcinomas. Carcinogenesis 2008; 29:1901–10.
16. Misawa A, Inoue J, Sugino Y, Hosoi H, Sugimoto T, Hosoda F, Ohki M, Imoto I, Inazawa J. Methylation-associated silencing of the nuclear receptor 1I2 gene in advanced-type neuroblastomas, identified by bacterial artificial chromosome array-based methylated CpG island amplification. Cancer Res 2005;65:10233–42.
17. Sugino Y, Misawa A, Inoue J, Kitagawa M, Hosoi H, Sugimoto T, Imoto I, Inazawa J. Epigenetic silencing of prostaglandin E receptor 2 (PTGER2) is associated with progression of neuroblastomas. Oncogene 2007;26:7401–13.
18. Tanaka K, Imoto I, Inoue J, Kozaki K, Tsuda H, Shimada Y, Aiko S, Yoshizumi Y, Iwai T, Kawano T, Inazawa J. Frequent methylation-associated silencing of a candidate tumor-suppressor. CRABP1, in esophageal squamous-cell carcinoma. Oncogene 2007;26:6456–68.
19. Inazawa J, Inoue J, Imoto I. Comparative genomic hybridization (CGH)-arrays pave the way for identification of novel cancer-related genes. Cancer Sci 2004;95:559–63.
20. Hirohashi S, Ishak KG, Kojiro M, Wanless IR, These ND, Tsukuma H, Blum HE, Deugnier Y, Puig PL, Fischer HP, Sakamoto M. Hepatocellular carcinoma. In: Hamilton SR, Altonen LA, eds. World Health Organization classification of tumours. Pathology and genetics. Tumours of the digestive system. Lyon: IARC Press, 2000. 159–72.
21. Estecio MR, Yan PS, Ibrahim AE, Tellez CS, Shen L, Huang TH, Issa JP. High-throughput methylation profiling by MCA coupled to CpG island microarray. Genome Res 2007;17:1529–36.
22. Jacinto FV, Ballestar E, Ropero S, Esteller M. Discovery of epigenetically silenced genes by methylated DNA immunoprecipitation in colon cancer cells. Cancer Res 2007;67:11481–6.
23. Nielander I, Bug S, Richter J, Giefing M, Martin-Subero JI, Siebert R. Combining array-based approaches for the identification of candidate tumor suppressor loci in mature lymphoid neoplasms. APMIS 2007;115:1107–34.
24. Maekita T, Nakazawa K, Mihara M, Nakajima T, Yanaoka K, Iguchi M, Arii K, Kaneda A, Tsukamoto T, Tatematsu M, Tamura G, Saito D, et al. High levels of aberrant DNA methylation in *Helicobacter pylori*-infected gastric mucosae and its possible association with gastric cancer risk. Clin Cancer Res 2006;12:989–95.
25. Frigola J, Song J, Stirzaker C, Hinshelwood RA, Peinado MA, Clark SJ. Epigenetic remodeling in colorectal cancer results in coordinate gene suppression across an entire chromosome band. Nat Genet 2006; 38:540–9.
26. Arai E, Ushijima S, Fujimoto H, Hosoda F, Shibata T, Kondo T, Yokoi S, Imoto I, Inazawa J, Hirohashi S, Kanai Y. Genome-wide DNA methylation profiles in both precancerous conditions and clear cell renal cell carcinomas are correlated with malignant potential and patient outcome. Carcinogenesis 2009;30:214–21.
27. Kanai Y, Ushijima S, Tsuda H, Sakamoto M, Hirohashi S. Aberrant DNA methylation precedes loss of heterozygosity on chromosome 16 in chronic hepatitis and liver cirrhosis. Cancer Lett 2000;148:73–80.
28. Kondo Y, Kanai Y, Sakamoto M, Mizokami M, Ueda R, Hirohashi S. Genetic instability and aberrant DNA methylation in chronic hepatitis and cirrhosis—A comprehensive study of loss of heterozygosity and microsatellite instability at 39 loci and DNA hypermethylation on 8 CpG islands in microdissected specimens from patients with hepatocellular carcinoma. Hepatology 2000;32:970–9.
29. Kanai Y, Saito Y, Ushijima S, Hirohashi S. Alterations in gene expression associated with the overexpression of a splice variant of DNA methyltransferase 3b, DNMT3b4, during human hepatocarcinogenesis. J Cancer Res Clin Oncol 2004;130:636–44.
30. Chang MH, Chen CJ, Lai MS, Hsu HM, Wu TC, Kong MS, Liang DC, Shau WY, Chen DS. Universal hepatitis B vaccination in Taiwan and the incidence of hepatocellular carcinoma in children. Taiwan Childhood Hepatoma Study Group. N Engl J Med 1997;336:1855–9.
31. Tanaka Y, Hanada K, Mizokami M, Yeo AE, Shih JW, Gojobori T, Alter HJ. Inaugural article: a comparison of the molecular clock of hepatitis C virus in the United States and Japan predicts that hepatocellular carcinoma incidence in the United States will increase over the next two decades. Proc Natl Acad Sci USA 2002;99:15584–9.
32. Park IY, Sohn BH, Yu E, Suh DJ, Chung YH, Lee JH, Surzycki SJ, Lee YI. Aberrant epigenetic modifications in hepatocarcinogenesis induced by hepatitis B virus X protein. Gastroenterology 2007; 132:1476–94.
33. Arase Y, Ikeda K, Suzuki F, Suzuki Y, Kobayashi M, Akuta N, Hosaka T, Sezaki H, Yatsuji H, Kawamura Y, Kobayashi M, Kumada H. Comparison of interferon and lamivudine treatment in Japanese patients with HBeAg positive chronic hepatitis B. J Med Virol 2007; 79:1286–92.
34. Yoshida H, Tateishi R, Arakawa Y, Sata M, Fujiyama S, Nishiguchi S, Ishibashi H, Yamada G, Yokosuka O, Shiratori Y, Omata M. Benefit of interferon therapy in hepatocellular carcinoma prevention for individual patients with chronic hepatitis C. Gut 2004;53:425–30.
35. Oikawa T, Ojima H, Yamasaki S, Takayama T, Hirohashi S, Sakamoto M. Multistep and multicentric development of hepatocellular carcinoma: histological analysis of 980 resected nodules. J Hepatol 2005;42:225–9.

Virchows Arch (2009) 454:513–517
DOI 10.1007/s00428-009-0762-6

ORIGINAL ARTICLE

Esophageal melanomas harbor frequent *NRAS* mutations unlike melanomas of other mucosal sites

Shigeki Sekine · Yukihiro Nakanishi · Reiko Ogawa · Satoko Kouda · Yae Kanai

Received: 4 January 2009 / Revised: 26 February 2009 / Accepted: 8 March 2009 / Published online: 25 March 2009

Abstract Mucosal melanomas have genetic alterations distinct from those in cutaneous melanomas. For example, *NRAS*- and *BRAF*-activating mutations occur frequently in cutaneous melanomas, but not in mucosal melanomas. We examined 16 esophageal melanomas for genetic alterations in *NRAS*, *BRAF*, and *KIT* to determine whether they exhibit genetic features common to melanomas arising from other mucosal sites. A sequencing analysis identified *NRAS* mutations in six cases; notably, four of these mutations were located in exon 1, an uncommon mutation site in cutaneous and other mucosal melanomas. *BRAF* and *KIT* mutations were found in one case each. Immunohistochemistry showed KIT expression in four cases, including the tumor with a *KIT* mutation and two other intramucosal tumors. The low frequency of *BRAF* mutations and the presence of a *KIT* mutation-positive case are findings similar to those of mucosal melanomas of other sites, but the prevalence of *NRAS* mutations was even higher than that of cutaneous melanomas. The present study implies that esophageal melanomas have genetic alterations unique from those observed in other mucosal melanomas.

Keywords *NRAS* · *BRAF* · *KIT* · Esophageal melanoma

Introduction

Melanomas show distinct patterns of genetic alterations depending on their sites of origin. The anatomical site-specific patterns of genetic alterations have been discussed in relation to the extent of ultraviolet exposure. *NRAS* and *BRAF* are the most frequently mutated oncogenes in melanomas. Both mutant N-Ras and B-Raf promote tumorigenesis through the constitutive activation of the MAP kinase pathway. Earlier studies suggested that *NRAS* mutations were frequent among melanomas arising from sun-exposed skin [1, 2]. Subsequently, *BRAF*-activating mutations were also identified in a significant proportion of melanomas [3]. Curtin et al. analyzed *NRAS* and *BRAF* mutations as well as DNA copy number changes in a large cohort of melanomas [4]. They utilized the presence of solar elastosis as a histological hallmark of chronic sun exposure and indicated that the majority of melanomas occurring on skin without chronic sun-induced damage had either *NRAS* or *BRAF* mutations whereas melanomas arising on skin with chronic sun-induced damage, acral sites, and mucosal membranes had mostly wild-type *NRAS* and *BRAF*. At the same time, they demonstrated that each group of melanomas exhibited distinct patterns of DNA copy number changes.

In addition to *NRAS* and *BRAF* mutations, a subset of melanomas contains *KIT* mutations [5–7]. Remarkably, the prevalence of *KIT* mutations also varies depending on the site of tumor origin, with the highest prevalence observed in mucosal melanomas [5]. Thus, genetic alterations in melanomas show site/organ-specific patterns and mucosal melanomas have distinct genetic features from those of cutaneous melanomas.

Esophageal melanomas are exceedingly rare, but highly aggressive neoplasms [8–10]. Previous studies have reported that melanomas constitute only 0.1–0.3% of all esophageal tumors [11, 12]. The rarity of this tumor is reasonable, considering the fact that the esophagus usually lacks melanocytes [13]. In addition, the esophagus is not

S. Sekine · Y. Nakanishi · R. Ogawa · S. Kouda · Y. Kanai (✉)
Pathology Division, National Cancer Center Research Institute,
5-1-1, Tsukiji, Chuo-ku,
Tokyo, Japan
e-mail: ykanai@ncc.go.jp

exposed to ultraviolet radiation, a major risk factor for melanomas. Because of the rarity of this lesion, data on genetic alterations in esophageal melanomas is scarce. However, the characterization of their genetic features, including how they differ from cutaneous melanomas and melanomas of other mucosal sites would contribute to the understanding of site/organ-specific genetic alterations in melanomas. Furthermore, considering the development of specific kinase inhibitors, such information could be critical for choosing an appropriate treatment. In this paper, we present the results of a mutational analysis of *NRAS*, *BRAF*, and *KIT* in 16 cases of esophageal melanomas.

Materials and methods

Sixteen surgically resected esophageal melanomas were examined in the present study (Table 1). The samples were routinely fixed with 10% formalin and embedded in paraffin. Five-micrometer-thick sections of each specimen were stained briefly with hematoxylin and eosin and used for DNA extraction. The tumor and nontumor areas were separately dissected using sterilized toothpicks under a microscope. Tissues obtained from the proper muscle layer distant from the tumors were used as nontumor samples. The dissected samples were incubated in 100 μL of DNA extraction buffer (50 mmol/L Tris–HCl, pH 8.0, 1 mmol/L ethylenediaminetetraacetic acid, 0.5% (*v*/*v*) Tween 20, 200 μg/mL proteinase K) at 37°C overnight. Proteinase K was inactivated by heating at 100°C for 10 min. The DNA samples were subjected to polymerase chain reaction (PCR) directly or after purification. When required, the samples were purified using a QIAquick PCR Purification Kit (Qiagen, Hilden, Germany). PCR was performed for 3 min at 95°C for initial denaturing, followed by 35 or 40 cycles at 94°C for 15 s, 58°C for 20 s, and 72°C for 60 s and a final extension at 72°C for 5 min. The primers that were used are listed in Table 2. The PCR products were electrophoresed in a 2% (*w*/*v*) agarose gel, visualized under UV light with ethidium bromide staining, and recovered using a QIAquick Gel Extraction Kit (Qiagen). Isolated PCR products were sequenced bidirectionally on an Applied Biosystems 3130 Genetic Analyzer (Applied Biosystems, Foster, CA, USA) using the same primers used for amplification. Each experiment, including DNA extraction, was done at least twice.

Immunohistochemical staining was performed using the avidin–biotin complex method. The primary antibody used was polyclonal anti-KIT (A4502; 1:100 dilution; Dako, Denmark). 3-3′-Diaminobenzidine tetrahydrochloride was used as a chromogen. The sections were counterstained with hematoxylin. Mast cells in the sections were used as positive controls. For negative controls, the tissue was processed in the same way but the primary antibody was omitted. The staining

Table 1 Results of mutational analysis and immunohistochemistry

Case no.	Age/sex	Depth of invasion	*BRAF*		*NRAS*		*KIT*		KIT IHC
			Nucleotide	Amino acid	Nucleotide	Amino acid	Nucleotide	Amino acid	
1	62/M	Mucosa	–		–		–		+++ (membranous)
2	67/M	Mucosa	–		–		–		+++ (membranous)
3	48/M	Submucosa	–		–		–		–
4	57/F	Submucosa	–		A183T	Q61H	–		–
5	64/M	Submucosa	–		–		–		–
6	67/M	Submucosa	–		–		–		–
7	72/M	Submucosa	–		G35C	G12A	–		–
8	73/M	Submucosa	–		–		–		–
9	48/M	Muscularis propria	–		–		C1727T	L576P	+++ (cytoplasmic)
10	68/M	Muscularis propria	T1799A	V600E	–		–		–
11	69/M	Muscularis propria	–		G34C	G12R	–		–
12	70/M	Muscularis propria	–		G38C	G13A	–		–
13	63/M	Adventitia	–		A183T	Q61H	–		–
14	64/M	Adventitia	–		–		–		–
15	68/M	Adventitia	–		G37C	G13R	–		–
16	71/M	Adventitia	–		–		–		++ (membranous)

IHC immunohistochemistry

Table 2 Primers used in the present study

	Forward primer	Reverse primer
BRAF exon15	TGTTTGCTCTGATAGGAAAATG	CTGATGGGACCCACTCCAT
NRAS exon 1	CAGGTTCTTGCTGGTGTGAAATGACTGAG	CTACCACTGGGCCTCACCTCTATGG
NRAS exon 2	AACAAGTGGTTATAGATGGTGA	CGTTAGAGGTTAATATCCGCA
KIT exon 11	TTTCCCTTTCTCCCCACAG	AAAGCCCCTGTTTCATACTGAC
KIT exon 13	TGCTAAAATGCATGTTTCCAAT	CAGCTTGGACACGGCTTTAC
KIT exon 17	TTTCTTTTCTCCTCCAACCTAA	TGTCAAGCAGAGAATGGGTACT

results were evaluated based on the amount of immunopositive tumor cells as follows: − [<5%], + [5–25%], ++ [25–75%], +++ [>75%]. When KIT is expressed, the staining intensity and the subcellular localization were also evaluated.

Results

The results of the mutational analysis are summarized in Table 1. A *BRAF* mutation was found in one case, while *NRAS* mutations were observed in six cases (Fig. 1). Four of six *NRAS* mutations were located in exon 1, and all these mutations were G to C transversions. All *BRAF* and *NRAS* mutations were missense mutations that had been previously identified as being oncogenic. A missense *KIT* mutation was observed in one case. The mutation affected the juxtamembrane domain of KIT. The wild-type sequence signal was very low for this mutation, suggesting that it was a homozygous mutation. All samples from nontumor areas showed wild-type sequences, indicating the somatic nature of the mutations. All the mutations that were observed were mutually exclusive.

Immunohistochemistry showed no or only focal and equivocal KIT expression in 12 cases (Fig. 2a). The case with the *KIT* mutation showed strong cytoplasmic expression (Fig. 2b), and another case showed heterogeneous staining with approximately 70% of the area exhibiting moderate membranous expression (Fig. 2c). Based on the heterogeneous KIT expression, we performed an additional mutational analysis. The KIT-positive and KIT-negative areas were separately subjected to sequencing analysis, but no *KIT* mutations were observed in either sample. Two early-stage melanomas limited to the mucosal layer exhibited strong and diffuse membranous KIT expression (Fig. 2d).

Discussion

NRAS and *BRAF* mutations are the most common genetic alterations in melanomas. An extensive literature review by Hocker and Tsao reported overall mutation rates of 26% for *NRAS* and 42% for *BRAF* in cutaneous melanomas [14]. In contrast, several studies concurred that these mutations are significantly less prevalent in mucosal melanomas with reported frequencies of 5–14% for *NRAS* and 0–10% for *BRAF* [2, 4, 15–17].

Our results showed that *BRAF* mutations are uncommon among esophageal melanomas as in mucosal melanomas of other organs. Unexpectedly, however, six of the 16 melanomas were found to harbor *NRAS*-activating mutations. While our series may not be sufficiently large to determine the mutational frequency conclusively, the prevalence of *NRAS* mutation-positive cases in the present series was even higher than that observed in cutaneous melanomas. Notably, four of the six mutations were located in exon 1 of *NRAS* and all these mutations were G to C transversions. This finding is intriguing as *NRAS* mutations in melanomas predominantly affect codon 61 within exon 2 and G to C transversion is a rare type of mutations for these sites [14].

Furthermore, previous studies showed that a few recurrent mutations are responsible for the vast majority of *NRAS* mutations in melanomas. The literature review by Hocker and Tsao showed that three mutations, G35A, C181A, and A182G, accounted for 82% of *NRAS* mutations of the 255 substitutions at the *NRAS* locus [14]. However, surprisingly, none of the six mutations identified in this study were identical to these most common *NRAS* mutations. These observations suggest that esophageal melanomas have a high frequency of *NRAS* mutations with a unique mutation spectrum.

Our literature review identified only one study analyzing *NRAS* and *BRAF* mutations in esophageal melanomas. Wong et al. examined three cases of esophageal melanomas, two of which had *NRAS*-activating mutations affecting codons 12 and 61, respectively [17]. On the other hand, only two *BRAF* and three *NRAS* mutations were identified in 33 mucosal melanomas arising outside of the esophagus in their series. While the number of subjects in their study was small, their result is consistent with our finding that esophageal melanomas have a high prevalence of *NRAS* mutations.

A *KIT* mutation was identified in one case, indicating that a subset of esophageal melanomas harbor *KIT*-activating mutations as in other mucosal melanomas. An identical mutation has been reported in gastrointestinal

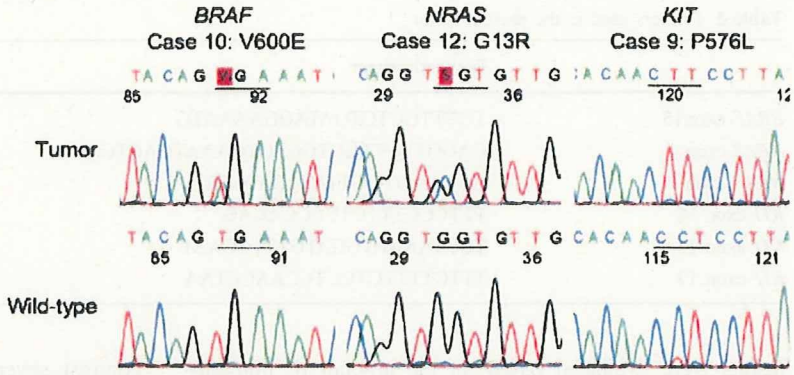

Fig. 1 Representative mutations of *BRAF*, *NRAS*, and *KIT* in esophageal melanomas. Heterozygous *BRAF* V600E and *NRAS* G13R mutations and homozygous P576L *KIT* mutation are shown

stromal tumors and anal melanomas [7, 18], and this mutation has been shown to be associated with a sensitivity to dasatinib and imatinib, inhibitors of SRC/ABL and KIT [7]. While the frequency of this mutation was not high in the present series, the identification of a *KIT* mutation is important, since it provides an immediate therapeutic application. Indeed, the successful treatments of melanomas with *KIT* mutations by imatinib have been recently reported [19, 20].

Of note, the case with the *KIT* mutation also exhibited the strong expression of KIT protein, whereas the majority of the mutation-negative melanomas did not express KIT, as determined using immunohistochemistry. This finding agrees with the results of previous studies on mucosal melanomas of other sites and suggests that immunohistochemistry is useful for excluding *KIT* mutation-negative cases prior to genetic testing [6, 7]. We also found KIT expression in two early-stage tumors. The expression of KIT in early-stage cutaneous melanomas has also been previously reported [21, 22]. Since non-neoplastic melanocytes express KIT, the expression of KIT in early-stage melanomas might be regarded as the retention of physiological expression in melanocytes [21]. Overall, our observations suggest that immunohistochemistry for KIT may be useful for prescreening *KIT* mutation-positive cases among advanced esophageal melanomas.

The present study indicates that esophageal melanomas have a high frequency of *NRAS* mutations unlike mucosal melanomas of other sites. Furthermore, the mutational spectrum of *NRAS* is distinct from those commonly observed in melanomas. Even among mucosal melanomas, the patterns of genetic alterations are likely distinct between

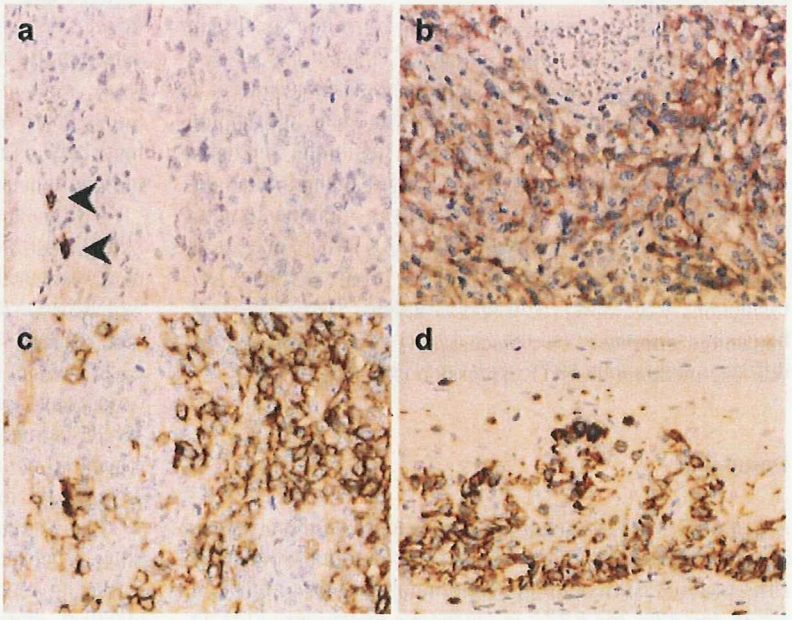

Fig. 2 KIT expression in esophageal melanomas. **a** This case lacks KIT expression. Few mast cells show positive staining (*arrowheads*; case 13). **b** Tumor cells show diffuse cytoplasmic staining (case 9). **c** An area of the tumor cells shows membranous expression (case 16). **d** Tumor cells proliferating within the epithelial layer show membranous expression (case 2)

differing sites of origin. Our observations also suggest that not only the degree of ultraviolet exposure, but also organ-specific factors may significantly influence the mutational spectrum in melanomas.

Acknowledgements This work was supported by a Grant-in-Aid for the Third Term Comprehensive 10-Year Strategy for Cancer Control, a Grant-in-Aid for Cancer Research from the Ministry of Health, Labor and Welfare of Japan, and a program for promotion of Fundamental Studies in Health Sciences of the National Institute of Biomedical Innovation (NiBio), Japan.

Conflicts of interest The authors declare that they have no conflicts of interest.

References

1. van't Veer LJ, Burgering BM, Versteeg R et al (1989) N-ras mutations in human cutaneous melanoma from sun-exposed body sites. Mol Cell Biol 9:3114–3116
2. Jiveskog S, Ragnarsson-Olding B, Platz A et al (1998) N-ras mutations are common in melanomas from sun-exposed skin of humans but rare in mucosal membranes or unexposed skin. J Invest Dermatol 111:757–761
3. Davies H, Bignell GR, Cox C et al (2002) Mutations of the BRAF gene in human cancer. Nature 417:949–954
4. Curtin JA, Fridlyand J, Kageshita T et al (2005) Distinct sets of genetic alterations in melanoma. N Engl J Med 353:2135–2147
5. Curtin JA, Busam K, Pinkel D et al (2006) Somatic activation of KIT in distinct subtypes of melanoma. J Clin Oncol 24:4340–4346
6. Rivera RS, Nagatsuka H, Gunduz M et al (2008) C-*kit* protein expression correlated with activating mutations in KIT gene in oral mucosal melanoma. Virchows Arch 452:27–32
7. Antonescu CR, Busam KJ, Francone TD et al (2007) L576P KIT mutation in anal melanomas correlates with KIT protein expression and is sensitive to specific kinase inhibition. Int J Cancer 121:257–264
8. Kato H, Watanabe H, Tachimori Y et al (1991) Primary malignant melanoma of the esophagus: report of four cases. Jpn J Clin Oncol 21:306–313
9. Li B, Lei W, Shao K et al (2007) Characteristics and prognosis of primary malignant melanoma of the esophagus. Melanoma Res 17:239–242
10. Lohmann CM, Hwu WJ, Iversen K et al (2003) Primary malignant melanoma of the oesophagus: a clinical and pathological study with emphasis on the immunophenotype of the tumours for melanocyte differentiation markers and cancer/testis antigens. Melanoma Res 13:595–601
11. Turnbull AD, Rosen P, Goodner JT et al (1973) Primary malignant tumors of the esophagus other than typical epidermoid carcinoma. Ann Thorac Surg 15:463–473
12. Scotto J, Fraumeni JF Jr, Lee JA (1976) Melanomas of the eye and other noncutaneous sites: epidemiologic aspects. J Natl Cancer Inst 56:489–491
13. Tateishi R, Taniguchi H, Wada A et al (1974) Argyrophil cells and melanocytes in esophageal mucosa. Arch Pathol 98:87–89
14. Hocker T, Tsao H (2007) Ultraviolet radiation and melanoma: a systematic review and analysis of reported sequence variants. Hum Mutat 28:578–588
15. Cohen Y, Rosenbaum E, Begum S et al (2004) Exon 15 BRAF mutations are uncommon in melanomas arising in nonsun-exposed sites. Clin Cancer Res 10:3444–3447
16. Edwards RH, Ward MR, Wu H et al (2004) Absence of BRAF mutations in UV-protected mucosal melanomas. J Med Genet 41:270–272
17. Wong CW, Fan YS, Chan TL et al (2005) BRAF and NRAS mutations are uncommon in melanomas arising in diverse internal organs. J Clin Pathol 58:640–644
18. Lasota J, Jasinski M, Sarlomo-Rikala M et al (1999) Mutations in exon 11 of c-*Kit* occur preferentially in malignant versus benign gastrointestinal stromal tumors and do not occur in leiomyomas or leiomyosarcomas. Am J Pathol 154:53–60
19. Hodi FS, Friedlander P, Corless CL et al (2008) Major response to imatinib mesylate in KIT-mutated melanoma. J Clin Oncol 26:2046–2051
20. Lutzky J, Bauer J, Bastian BC (2008) Dose-dependent, complete response to imatinib of a metastatic mucosal melanoma with a K642E KIT mutation. Pigment Cell Melanoma Res 21:492–493
21. Montone KT, van Belle P, Elenitsas R et al (1997) Proto-oncogene c-*kit* expression in malignant melanoma: protein loss with tumor progression. Mod Pathol 10:939–944
22. Janku F, Novotny J, Julis I et al (2005) KIT receptor is expressed in more than 50% of early-stage malignant melanoma: a retrospective study of 261 patients. Melanoma Res 15:251–256

Journal of Pathology
J Pathol 2009; **219**: 365–372
Published online 27 July 2009 in Wiley InterScience
(www.interscience.wiley.com) **DOI:** 10.1002/path.2606

Original Paper

Dicer is required for proper liver zonation

Shigeki Sekine,[1]* Reiko Ogawa,[1] Michael T Mcmanus,[2] Yae Kanai[1] and Matthias Hebrok[2]
[1]*Pathology Division, National Cancer Center Research Institute, Tokyo, Japan*
[2]*Diabetes Center, Department of Medicine, University of California San Francisco, San Francisco, California, USA*

**Correspondence to:*
Shigeki Sekine, Pathology Division, National Cancer Center Research Institute, 5-1-1, Tsukiji, Chuo-ku, Tokyo, Japan.
E-mail: ssekine@ncc.go.jp

No conflicts of interest were declared.

Received: 21 June 2009
Revised: 17 July 2009
Accepted: 17 July 2009

Abstract

A number of genes and their protein products are expressed within the liver lobules in a region-specific manner and confer heterogeneous metabolic properties to hepatocytes; this phenomenon is known as 'metabolic zonation'. To elucidate the roles of Dicer, an endoribonuclease III type enzyme required for microRNA biogenesis, in the establishment of liver zonation, we examined the distribution of proteins exhibiting pericentral or periportal localization in hepatocyte-specific *Dicer1* knockout mouse livers. Immunohistochemistry showed that the localization of pericentral proteins was mostly preserved in *Dicer1*-deficient livers. However, glutamine synthetase, whose expression is normally confined to a few layers of hepatocytes surrounding the central veins, was expressed in broader pericentral areas. Even more striking was the observation that all the periportal proteins that were examined, including phosphoenolpyruvate carboxykinase, E-cadherin, arginase 1, and carbamoyl phosphate synthetase-I, lost their localized expression patterns and were diffusely expressed throughout the entire lobule. Thus, with regard to periportal protein expression, the consequences of Dicer loss were similar to those caused by the disruption of β-catenin. An analysis of livers deficient in β-catenin did not identify the down-regulation of *Dicer1* or any microRNAs, indicating that they are not directly activated by β-catenin. Thus, the present study illustrates that Dicer plays a pivotal role in the establishment of liver zonation. Dicer is essential for the suppression of periportal proteins by Wnt/β-catenin/TCF signalling, albeit it likely acts in an indirect manner.

Keywords: Dicer; β-catenin; liver; zonation

Introduction

Although hepatocytes are uniform at a histological level, they differ in a number of metabolic functions [1,2]. For example, pericentral hepatocytes are active in glutamine and bile acid synthesis and the metabolism of xenobiotics, whereas periportal hepatocytes are more active in cholesterol, urea, and glucose synthesis [1,2]. The metabolic heterogeneity of hepatocytes enables multiple and occasionally antagonistic metabolic functions to be performed efficiently in the liver. A number of genes and their protein products involved in these metabolic processes are expressed in a region-specific manner along the porto-central axis within the liver lobule and their respective functions confer the heterogeneous metabolic properties of hepatocytes [1–3].

Recent studies have revealed that the Wnt signalling pathway plays a key role in the establishment of liver zonation [4,5]. The Wnt signalling pathway is activated by the binding of secreted Wnt ligands to Frz and Lrp receptors on cell membranes. This leads to the stabilization of β-catenin through the inhibition of proteosomal degradation, and the translocation of the protein to the nucleus, where it activates TCF-dependent transcription [6]. β-Catenin/TCF-dependent transcription is normally active in the pericentral hepatocytes, where it induces pericentral gene expression while suppressing periportal gene expression [4,7]. The hepatocyte-specific ablation of Apc, leading to the constitutive activation of β-catenin/TCF-dependent transcription, resulted in the diffuse expression of pericentral genes and the down-regulation of periportal genes throughout the entire liver lobule [4,8]. Conversely, the suppression of Wnt signalling by the overexpression of Dkk1 or the conditional ablation of β-catenin caused a loss of pericentral gene expression and the diffuse expression of periportal genes [4,9]. Braeuning *et al* further showed that activation of the Ras/MAPK pathway by the oncogenic form of H-ras or serum components suppressed pericentral genes and induced periportal genes through the inhibition of β-catenin/TCF-dependent transcription [10,11]. Thus, the expression of pericentral and periportal genes is coordinately and inversely regulated by Wnt/β-catenin/TCF signalling.

Dicer is an essential component of microRNA biogenesis that cleaves pre-microRNAs into mature microRNAs. Since Dicer is encoded by a single locus in the mouse genome, the disruption of the single *Dicer1* gene results in the loss of virtually all microRNAs [12–14]. Here, we demonstrate that Dicer plays an essential role in the establishment of proper liver zonation. Remarkably, the loss of Dicer impairs the localization of periportal proteins, leaving the expression of pericentral proteins mostly intact. Thus, our results reveal the novel finding that microRNAs appear to be specifically required for the suppression of periportal protein expression.

Materials and methods

Mice

Alb-Cre [15,16], *Dicer1*$^{flox/flox}$ [12], *Ctnnb1*$^{flox/flox}$ [17], *Alb-Cre;Ctnnb1*$^{flox/flox}$ [7,9], and *Alb-Cre;Dicer*$^{flox/flox}$ [18] mice have been previously described. The mice used in the present study were maintained in barrier facilities and all studies were conducted in compliance with the University of California IACUC (Institutional Animal Care and Use Committee) guidelines and according to protocols approved by the Committee for Ethics in Animal Experimentation at the National Cancer Center, Japan.

Immunohistochemistry

Liver tissue samples were fixed with 10% buffered formalin, embedded in paraffin, and cut into 5-μm-thick sections. Immunohistochemistry was performed by an indirect immunoperoxidase method using peroxidise-labelled anti-mouse, -rabbit or -goat polymers (Histofine Simple Stain, Nichirei, Tokyo, Japan). 3,3′-Diaminobenzidine tetrahydrochloride was used as a chromogen. The primary antibodies that were used are listed in Table 1. For double immunofluorescence staining, anti-mouse IgG antibody conjugated with Alexa Fluor 488 and anti-rabbit IgG antibody conjugated with Alexa Fluor 594 were used as secondary antibodies. The sections were analysed using a confocal microscope (LSM5 Pascal; Carl Zeiss Jena GmbH, Jena, Germany) equipped with a 15 mW Kr/Ar laser.

Quantitative PCR

RNA extraction and the reverse-transcription reaction were performed using standard protocols. Quantitative PCR reactions were performed using SYBR Green PCR master mix (Applied Biosystems, CA, USA). The expression of *Dicer1* was compared with the expression level of *Gusb*, as previously described [9]. The primer sequences were as follows: *Dicer1*: GAACGAAATGCAAGGAATGGA and GGGACTTCGATATCCTCTTCTTTCTC; *Gusb*: ACGGGATTGTGGTCATCGA and TCGTTGCCAAAACTCTGAGGTA.

Microarray analysis

RNA samples were prepared from liver tissues of 6-week-old female *Alb-Cre;Ctnnb1*$^{flox/flox}$ and *Ctnnb1*$^{flox/flox}$ mice. The samples were labelled with a miRNA Labeling Reagent & Hybridization Kit (Agilent Technologies, CA, USA) based on the manufacturer's instructions. The labelled RNA samples were hybridized with a mouse miRNA microarray (Agilent Technologies) containing 566 mouse miRNA probes based on Sanger miRBase v10.0. MicroRNAs that showed more than two-fold changes with $p < 0.05$ (Welch t-test) were considered significant.

Results

Localization of pericentral proteins is only marginally affected in Dicer mutant mice

To elucidate the roles of Dicer in liver zonation, liver samples from *Alb-Cre;Dicer*$^{flox/flox}$ mice and their control littermates (*Dicer*$^{flox/flox}$) were immunohistochemically examined. As previously reported, the efficient deletion of *Dicer1* in hepatocytes was achieved in 3-week-old *Alb-Cre;Dicer*$^{flox/flox}$ mice; however, *Dicer1*-deficient hepatocytes were prone to apoptosis and the complete disruption of *Dicer1* was followed by repopulation with *Dicer1*-expressing hepatocytes that had escaped Cre-mediated recombination [18]. We therefore examined the livers from 3-week-old *Alb-Cre;Dicer*$^{flox/flox}$ and *Dicer*$^{flox/flox}$ mice (hereafter referred to as Dicer-deficient and control livers).

Immunohistochemistry showed that the localization of pericentral proteins was mostly maintained

Table 1. Antibodies used for immunohistochemistry

Antigen	Clone	Dilution	Source
Glutamine synthetase	6	1:1000	Becton Dickinson, Franklin Lakes, USA
GLT-1	Polyclonal	1:500	Dr Masahiko Watanabe [24]
OAT	Polyclonal	1:500	Santa Cruz Biotechnologies, Santa Cruz, USA
CYP2E1	Polyclonal	1:500	Dr Magnus Ingelman-Sundberg [25]
E-cadherin	36	1:250	Becton Dickinson, Franklin Lakes, USA
PEPCK	Polyclonal	1:200	Santa Cruz Biotechnologies, Santa Cruz, USA
CPS1	Polyclonal	1:500	Santa Cruz Biotechnologies, Santa Cruz, USA
Arginase I	19	1:2500	Becton Dickinson, Franklin Lakes, USA

OAT = ornithine aminotransferase; PEPCK = phosphoenolpyruvate carboxykinase; CPS1 = carbamoyl phosphate synthetase-I.

in the absence of Dicer. The distributions of GLT-1, ornithine aminotransferase (OAT), and CYP2E1 were unaltered in Dicer-deficient livers. GLT-1 and OAT were expressed in a few layers of hepatocytes surrounding the central veins (Figures 1A, 1B, 1D, and 1E). CYP2E1 was expressed in broader pericentral areas (Figures 1J and 1K). Expression of glutamine synthetase (GS) was observed in the pericentral areas of both mice; however, the GS-positive areas were significantly broader in the Dicer-deficient livers (Figures 1G and 1H).

The altered localization of GS was confirmed by double immunofluorescence staining for GS and CYP2E1. In control mouse livers, distinct distributions of these proteins were evident: GS expression was restricted to a few layers of hepatocytes surrounding the central veins, whereas CYP2E1 expression was extended to the distal pericentral

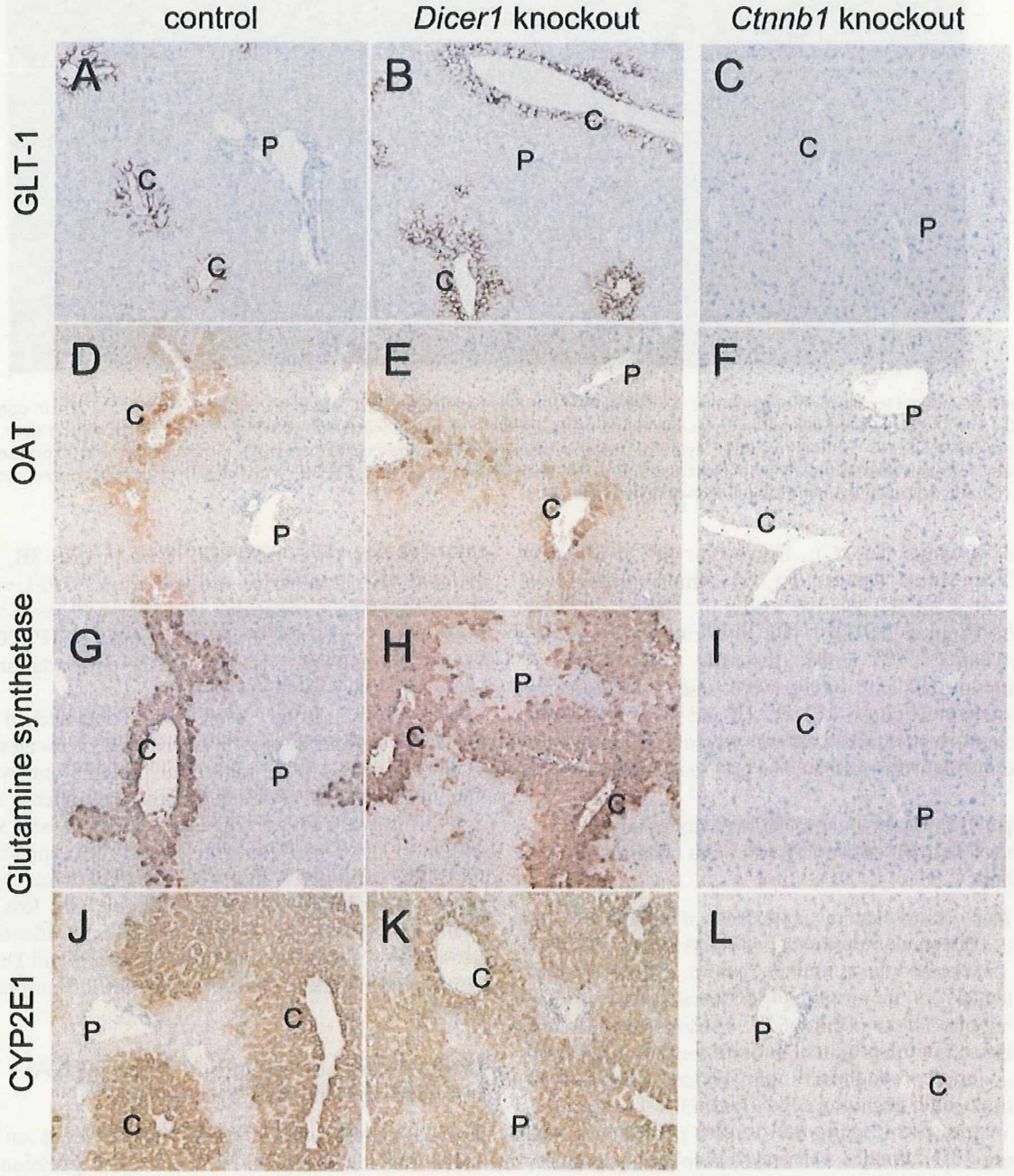

Figure 1. Expression of pericentral proteins in Dicer-deficient liver. Pericentral protein expression was examined using immunohistochemistry. The distributions of GLT-1, OAT, and CYP2E1 were unaltered in Dicer-deficient liver (B, E, K) compared with those in control mouse liver (*Dicer*$^{flox/flox}$) (A, D, J). Glutamine synthetase maintained its pericentral localization in Dicer-deficient liver (H), but its expression extended beyond its normal boundary and encompassed a broader area than that observed in control mouse liver (G). Pericentral protein expression was completely lost in β-catenin-deficient livers (C, F, I, L). C = pericentral vein; P = portal tract

J Pathol 2009; **219**: 365–372 DOI: 10.1002/path

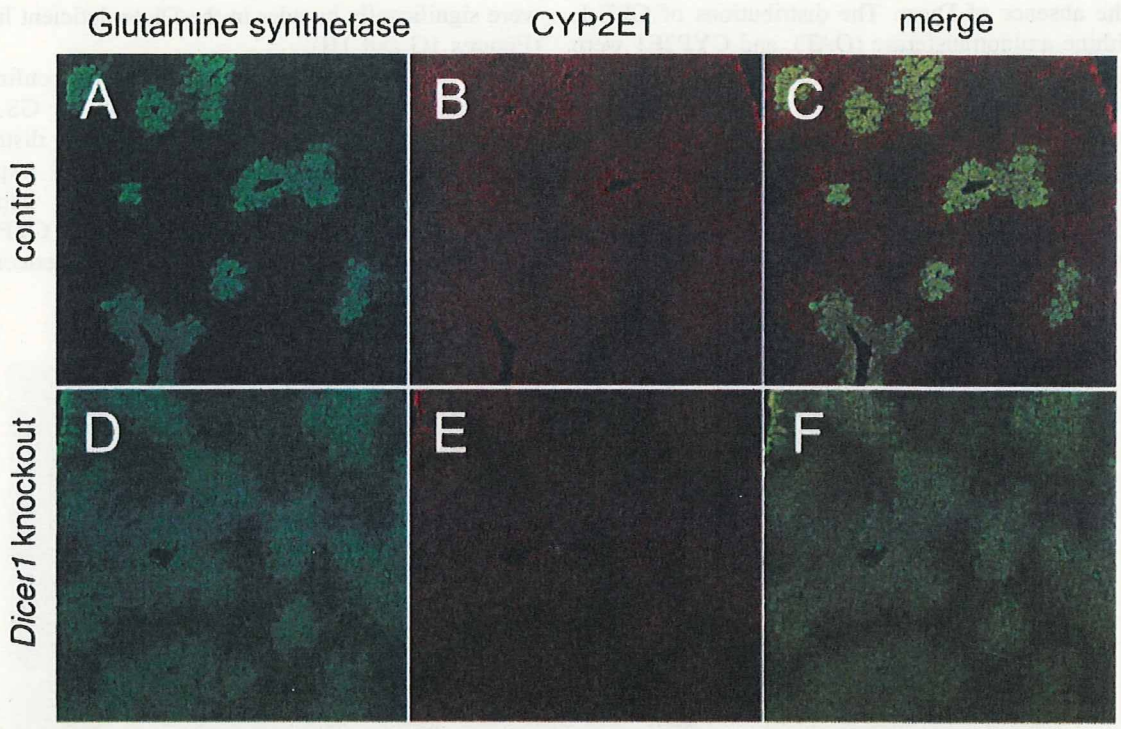

Figure 2. Altered localization of glutamine synthetase (GS) in Dicer-deficient liver. The expression of GS and CYP2E1 in control (A–C) and Dicer-deficient liver (D–F) was examined using double immunofluorescence staining. In the control mouse liver, the expression of GS was confined to a few layers of hepatocytes surrounding the central veins (A). However, GS was expressed in broader pericentral areas in Dicer-deficient livers (D). The distributions of GS and CYP2E1 were clearly distinct in control mouse liver (C) but were almost identical in Dicer-deficient liver (F)

areas (Figures 2A–2C). However, the distribution of GS-positive hepatocytes was almost identical to that of CYP2E1-positive cells in *Dicer1*-deficient livers (Figures 2D–2F). The liver tissues from *Alb-Cre;Ctnnb1*$^{flox/flox}$ mice (hereafter referred to as β-catenin-deficient livers) were also examined for comparison (Figures 1C, 1F, 1H, and 1K). β-Catenin-deficient livers lost the expression of all the pericentral proteins that were examined as previously reported [9].

Periportal proteins are diffusely expressed throughout the entire lobule in the absence of Dicer

We then examined the expression of periportal proteins. Phosphoenolpyruvate carboxykinase (PEPCK) was expressed in a gradient pattern, with the highest levels in the proximal periportal areas in control mouse livers (Figure 3A). E-cadherin was also expressed in the proximal periportal regions but exhibited a more pronounced sharp demarcation between positive and negative cells (Figure 3D). Arginase 1 was expressed in periportal to distal pericentral areas (Figure 3G). Finally, carbamoyl phosphate synthetase-I (CPS1) expression was found throughout the liver lobules, with the exception of a few layers of perivenous hepatocytes; this distribution was complementary to that of GS (Figure 3J). Remarkably, all of these periportal proteins lost their localized expression patterns and appeared in a diffuse pattern throughout the entire lobule in Dicer-deficient livers (Figures 3B, 3E, 3H, and 3K). E-cadherin, arginase 1, and CPS1 were all homogeneously expressed in all hepatocytes. Some heterogeneity was noted in the staining for PEPCK, but the predominant expression in the periportal areas was lost in Dicer-deficient livers.

Interestingly, similar results were obtained in an analysis of periportal protein expression in β-catenin-deficient livers. All the periportal proteins that were examined lost their restricted expression patterns and were diffusely expressed (Figures 3C, 3F, 3I, and 3L). Similar to the Dicer-deficient livers, the expression of PEPCK exhibited minor heterogeneity. Thus, with regard to periportal protein expression, the loss of β-catenin and Dicer resulted in virtually identical phenotypes, suggesting that both β-catenin and Dicer are required for the localized expression of periportal proteins.

Neither *Dicer1* nor any individual microRNAs are directly activated by β-catenin/TCF

Previous studies and the present observations on β-catenin-deficient livers showed that the expression of pericentral proteins is dependent on active Wnt/β-catenin signalling [4,9]. The conserved pericentral protein expression therefore indicates that Wnt signalling is still active in the pericentral hepatocytes of Dicer-deficient livers. On the other hand, periportal proteins are diffusely expressed throughout the liver lobules in

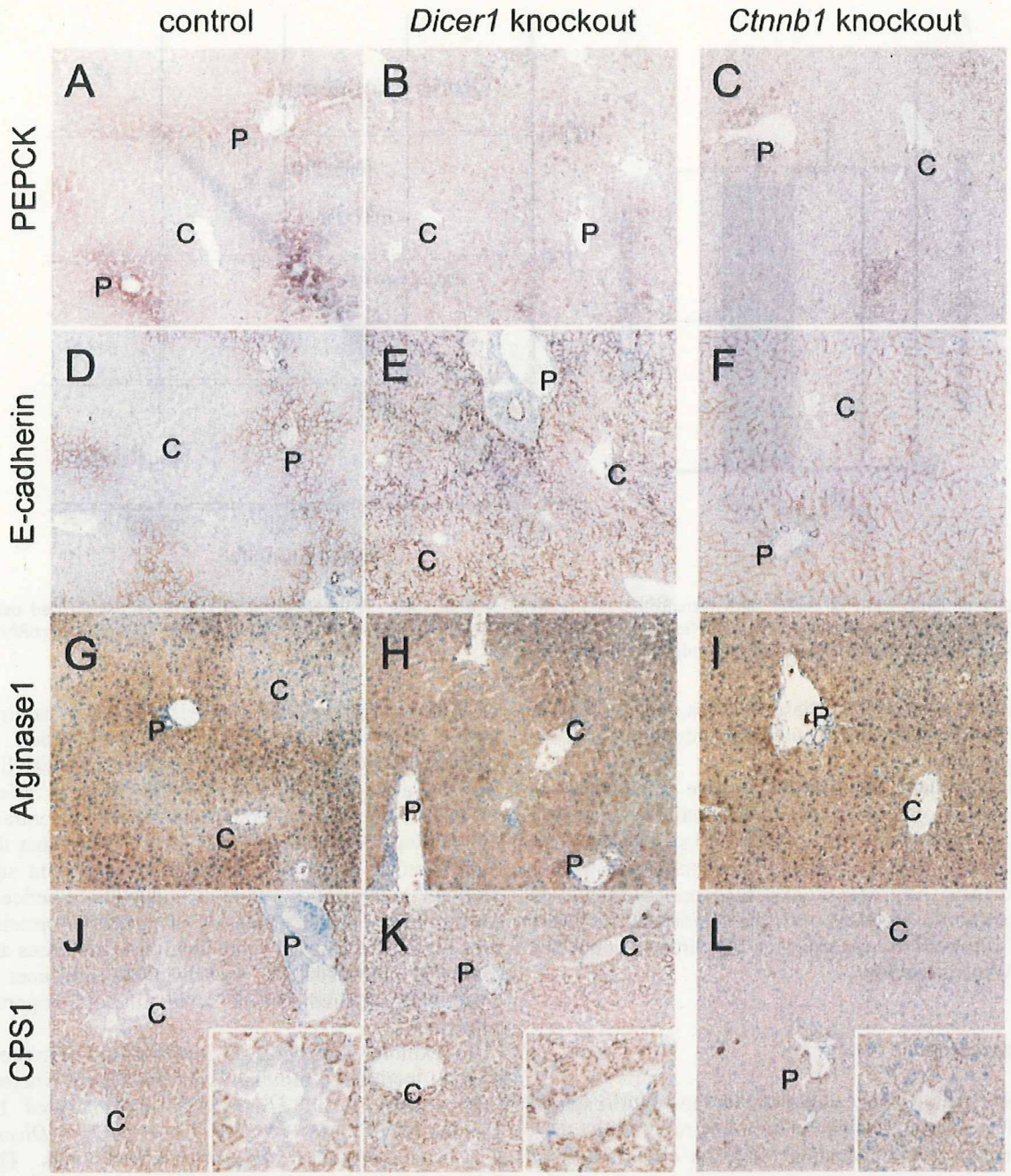

Figure 3. Expression of periportal proteins in Dicer-deficient liver. Periportal protein expression was examined using immunohistochemistry. The characteristic distributions of the periportal proteins in the control mouse liver (A, D, G, J) were completely lost in the Dicer-deficient (B, E, H, K) and β-catenin-deficient livers (C, F, I, L). High-magnification views of the pericentral areas are presented as insets for CPS1 (J–L). C = pericentral vein; P = portal tract

Dicer-deficient livers. This finding suggests that Dicer is essential for the repression of periportal proteins achieved by active Wnt signalling and that Dicer may act downstream of β-catenin/TCF. However, *Dicer1* expression was not affected in β-catenin-deficient livers, indicating that *Dicer1* itself is not involved immediately downstream of Wnt signalling (Figure 4A).

Furthermore, we performed a microarray analysis to test whether individual microRNAs are regulated by β-catenin. Similarly, a comparison of β-catenin-deficient and control livers identified no microRNAs whose expression levels were down-regulated in β-catenin-deficient livers. Thus, we did not find any microRNAs that were directly activated by β-catenin/TCF signalling (Figure 4B and Supporting information, Supplementary Table 1). On the other hand, the analysis identified four microRNAs that were up-regulated in β-catenin-deficient livers: miR-31 (2.84-fold), miR-34a (2.77-fold), miR-31* (2.91-fold), and miR-193b (2.21-fold). However, considering the modest increase

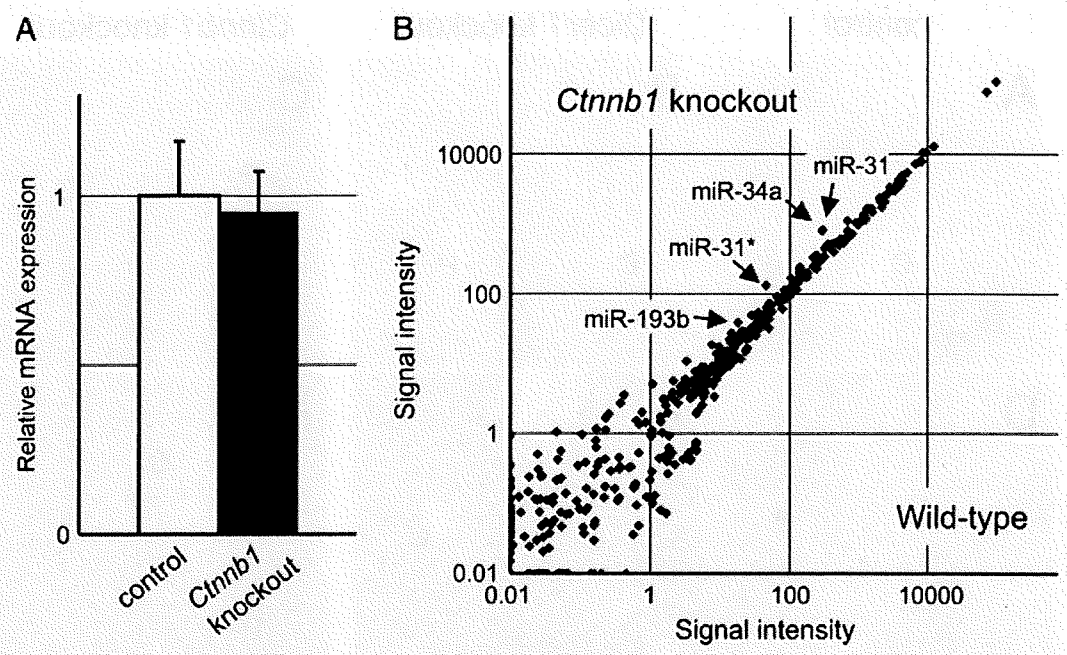

Figure 4. Expression of *Dicer1* and microRNAs in β-catenin-deficient liver. (A) Expression of *Dicer1* as determined using quantitative PCR ($n = 6$ per group). (B) Microarray analysis of microRNA expression ($n = 3$ per group). The four microRNAs with significantly altered expressions are indicated by the arrows

of these microRNAs, these changes are unlikely to explain the dramatically altered expression of periportal proteins.

In summary, our data demonstrate that neither the expression of *Dicer1* nor that of individual microRNAs is dependent on β-catenin/TCF signalling. Thus, while Dicer and β-catenin elimination results in similar defects with regard to the inappropriate expression of periportal proteins, our results indicate that Dicer and microRNA expression is not directly controlled by Wnt signalling.

Discussion

Recent studies have suggested that the Wnt/β-catenin/TCF signalling pathway plays a key role in the establishment of liver zonation [4,5]. As observations of β-catenin-deficient liver have indicated, β-catenin-mediated signalling is essential for both the expression of pericentral proteins and the repression of periportal proteins in pericentral hepatocytes. Even though MAPK signalling has been reported to affect zonation through the modulation of β-catenin/TCF-dependent transcription [11], the mechanisms underlying the establishment of zonation remain largely undefined. The present study identified Dicer as a novel and essential component in the establishment of one aspect of liver zonation, the repression of periportal proteins in pericentral areas.

The hepatocyte-specific loss of Dicer resulted in the diffuse expression of proteins that are normally localized to the periportal areas. On the other hand, the localization of pericentral proteins was left mostly unaltered. Since pericentral protein expression requires active Wnt signalling [4,8,9], the conservation of pericentral protein expression in Dicer-deficient livers indicates that the loss of Dicer does not affect Wnt activity in pericentral hepatocytes. In contrast, our findings in Dicer-deficient livers suggest that the repression of periportal proteins by active Wnt signalling requires Dicer. While the induction of pericentral proteins and the repression of periportal proteins are coordinated by Wnt signalling, these processes are regulated independently of each other, and Dicer is selectively required for the repression of periportal proteins.

To explore how Dicer is involved in the repression of periportal proteins, we first tested whether the expression of Dicer itself was regulated by β-catenin/TCF; however, the expression of *Dicer1* was not altered in β-catenin-deficient livers. The primary physiological role of Dicer is microRNA processing [12,19]. While Dicer has microRNA-independent functions, such as endogenous siRNA processing in at least some organs [20,21], Dicer's functions are generally thought to be largely mediated by microRNAs. Since microRNA precursors are mostly transcribed by RNA polymerase II [22], some microRNAs might be transactivated by β-catenin/TCF, resulting in suppression of periportal genes. Nevertheless, we could not identify any microRNAs that were down-regulated in β-catenin-deficient livers. Collectively, these observations imply that Dicer plays an essential role in the repression of periportal proteins at some point downstream of β-catenin/TCF signalling, albeit this effect likely occurs through an indirect mechanism.

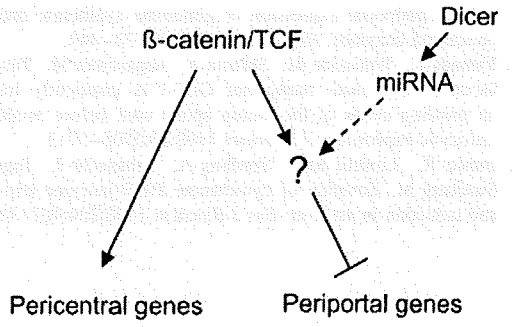

Figure 5. Model of the regulation of zonal gene expression. β-Catenin/TCF transactivates pericentral genes as well as represses periportal genes. Dicer and microRNAs are essential for the repression of periportal genes, but are not directly regulated by β-catenin

The disruption of Dicer did not have a major effect on the localization of pericentral proteins, but it did result in the expression of GS in a broader area. This finding indicates that a suppressive signal mediated by Dicer is required for the repression of GS in distal pericentral areas. A previous study reported that loss of Hnf4a also caused aberrant GS expression [23]. However, the loss of Hnf4a resulted in weak expression of GS in the entire lobule, unlike in Dicer-deficient livers, and the expression of Hnf4a was not altered in Dicer-deficient livers [18]. While the loss of Dicer and Hnf4a both affected the localization of GS, these two molecules seem to regulate GS expression through independent mechanisms.

In summary, the present study shows that Dicer is required for the establishment of proper liver zonation. Dicer is essential for the suppression of periportal proteins by Wnt/β-catenin/TCF signalling, albeit neither Dicer itself nor any individual microRNAs are directly activated by β-catenin/TCF. Our results suggest that Dicer regulates factor(s) that suppress periportal genes at some point downstream of β-catenin (Figure 5). However, the individual microRNAs responsible for the repression of periportal proteins remain elusive at present. Further studies of individual microRNAs should help to elucidate the precise mechanisms by which these factors regulate zonal gene expression in the liver.

Acknowledgements

We thank Ms Kaho Minoura (Agilent Technologies) for the microRNA analysis, Dr Magnus Ingelman-Sundberg (Karolinska Institute, Stockholm, Sweden) and Dr Masahiko Watanabe (Hokkaido University, Sapporo, Japan) for providing antibodies, and Mr Shigeru Tamura for photographic assistance. This work was supported by KAKENHI (20790315) from the Ministry of Education, Culture, Sports, Science and Technology, Japan, and a Grant-in-Aid for the Third Term Comprehensive 10-Year Strategy for Cancer Control and a Grant-in-Aid for Cancer Research from the Ministry of Health, Labour, and Welfare of Japan. Work in MH's laboratory was supported by a NIH grant (CA112537).

References

1. Jungermann K, Kietzmann T. Zonation of parenchymal and nonparenchymal metabolism in liver. *Annu Rev Nutr* 1996;**16:**179–203.
2. Gebhardt R. Metabolic zonation of the liver: regulation and implications for liver function. *Pharmacol Ther* 1992;**53:**275–354.
3. Braeuning A, Ittrich C, Kohle C, Hailfinger S, Bonin M, Buchmann A, *et al.* Differential gene expression in periportal and perivenous mouse hepatocytes. *FEBS J* 2006;**273:**5051–5061.
4. Benhamouche S, Decaens T, Godard C, Chambrey R, Rickman DS, Moinard C, *et al.* Apc tumor suppressor gene is the 'zonation-keeper' of mouse liver. *Dev Cell* 2006;**10:**759–770.
5. Hailfinger S, Jaworski M, Braeuning A, Buchmann A, Schwarz M. Zonal gene expression in murine liver: lessons from tumors. *Hepatology* 2006;**43:**407–414.
6. Gordon MD, Nusse R. Wnt signaling: multiple pathways, multiple receptors, and multiple transcription factors. *J Biol Chem* 2006;**281:**22429–22433.
7. Sekine S, Gutierrez P, Lan B, Feng S, Hebrok M. Liver specific loss of beta-catenin results in delayed hepatocyte proliferation after partial hepatectomy. *Hepatology* 2007;**45:**361–368.
8. Colnot S, Decaens T, Niwa-Kawakita M, Godard C, Hamard G, Kahn A, *et al.* Liver-targeted disruption of Apc in mice activates beta-catenin signaling and leads to hepatocellular carcinomas. *Proc Natl Acad Sci U S A* 2004;**101:**17216–17221.
9. Sekine S, Lan BY, Bedolli M, Feng S, Hebrok M. Liver-specific loss of beta-catenin blocks glutamine synthesis pathway activity and cytochrome p450 expression in mice. *Hepatology* 2006;**43:**817–825.
10. Braeuning A, Ittrich C, Koehle C, Buchmann A, Schwarz M. Zonal gene expression in mouse liver resembles expression patterns of Ha-ras and {beta}-catenin mutated hepatomas. *Drug Metab Dispos* 2007;**35:**503–507.
11. Braeuning A, Menzel M, Kleinschnitz EM, Harada N, Tamai Y, Kohle C, *et al.* Serum components and activated Ha-ras antagonize expression of perivenous marker genes stimulated by beta-catenin signaling in mouse hepatocytes. *FEBS J* 2007;**274:**4766–4777.
12. Harfe BD, McManus MT, Mansfield JH, Hornstein E, Tabin CJ. The RNaseIII enzyme Dicer is required for morphogenesis but not patterning of the vertebrate limb. *Proc Natl Acad Sci U S A* 2005;**102:**10898–10903.
13. Murchison EP, Partridge JF, Tam OH, Cheloufi S, Hannon GJ. Characterization of Dicer-deficient murine embryonic stem cells. *Proc Natl Acad Sci U S A* 2005;**102:**12135–12140.
14. Kanellopoulou C, Muljo SA, Kung AL, Ganesan S, Drapkin R, Jenuwein T, *et al.* Dicer-deficient mouse embryonic stem cells are defective in differentiation and centromeric silencing. *Genes Dev* 2005;**19:**489–501.
15. Postic C, Shiota M, Niswender KD, Jetton TL, Chen Y, Moates JM, *et al.* Dual roles for glucokinase in glucose homeostasis as determined by liver and pancreatic beta cell-specific gene knock-outs using Cre recombinase. *J Biol Chem* 1999;**274:**305–315.
16. Postic C, Magnuson MA. DNA excision in liver by an albumin-Cre transgene occurs progressively with age. *Genesis* 2000;**26:**149–150.
17. Brault V, Moore R, Kutsch S, Ishibashi M, Rowitch DH, McMahon AP, *et al.* Inactivation of the beta-catenin gene by Wnt1-Cre-mediated deletion results in dramatic brain malformation and failure of craniofacial development. *Development* 2001;**128:**1253–1264.
18. Sekine S, Ogawa R, Ito R, Hiraoka N, McManus MT, Kanai Y, *et al.* Disruption of Dicer1 induces dysregulated fetal gene expression and promotes hepatocarcinogenesis. *Gastroenterology* 2009;**136:**2304–2315.
19. Calabrese JM, Seila AC, Yeo GW, Sharp PA. RNA sequence analysis defines Dicer's role in mouse embryonic stem cells. *Proc Natl Acad Sci U S A* 2007;**104:**18097–18102.
20. Tam OH, Aravin AA, Stein P, Girard A, Murchison EP, Cheloufi S, *et al.* Pseudogene-derived small interfering RNAs regulate gene expression in mouse oocytes. *Nature* 2008;**453:**534–538.

21. Watanabe T, Totoki Y, Toyoda A, Kaneda M, Kuramochi-Miyagawa S, Obata Y, *et al.* Endogenous siRNAs from naturally formed dsRNAs regulate transcripts in mouse oocytes. *Nature* 2008;**453**:539–543.
22. Lee Y, Kim M, Han J, Yeom KH, Lee S, Baek SH, *et al.* MicroRNA genes are transcribed by RNA polymerase II. *EMBO J* 2004;**23**:4051–4060.
23. Stanulovic VS, Kyrmizi I, Kruithof-de Julio M, Hoogenkamp M, Vermeulen JL, Ruijter JM, *et al.* Hepatic HNF4alpha deficiency induces periportal expression of glutamine synthetase and other pericentral enzymes. *Hepatology* 2007;**45**:433–444.
24. Yamada K, Watanabe M, Shibata T, Nagashima M, Tanaka K, Inoue Y. Glutamate transporter GLT-1 is transiently localized on growing axons of the mouse spinal cord before establishing astrocytic expression. *J Neurosci* 1998;**18**:5706–5713.
25. Buhler R, Lindros KO, Nordling A, Johansson I, Ingelman-Sundberg M. Zonation of cytochrome P450 isozyme expression and induction in rat liver. *Eur J Biochem* 1992;**204**:407–412.

SUPPORTING INFORMATION ON THE INTERNET

The following supporting information may be found in the online version of this article.

Table S1. MicroRNA expression in β-catenin-deficient liver

J Pathol 2009; **219**: 365–372 DOI: 10.1002/path

Intraductal carcinoma component as a favorable prognostic factor in biliary tract carcinoma

Hidenori Ojima,[1] Yae Kanai,[1,5] Motoki Iwasaki,[2] Nobuyoshi Hiraoka,[1] Kazuaki Shimada,[3] Tsuyoshi Sano,[3] Yoshihiro Sakamoto,[3] Minoru Esaki,[3] Tomoo Kosuge,[3] Michiie Sakamoto[4] and Setsuo Hirohashi[1]

[1]Pathology Division, National Cancer Center Research Institute, [2]Epidemiology and Prevention Division, Research Center for Cancer Prevention and Screening, National Cancer Center, [3]Hepatobiliary and Pancreatic Surgery Division, National Cancer Center Hospital, 5-1-1 Tsukiji, Chuo-ku, Tokyo 104-0045; [4]Department of Pathology, Keio University School of Medicine, 35 Shinanomachi, Shinjyuku-ku, Tokyo 160-0016, Japan

(Received July 5, 2008/Revised September 9, 2008/Accepted September 16, 2008/Online publication November 25, 2008)

The aim of this study is to evaluate the prognostic impact of an intraductal carcinoma component and bile duct resection margin status in patients with biliary tract carcinoma. An intraductal carcinoma component was defined as carcinoma within the bile duct outside the main tumor nodule consisting of a subepithelial invasive component. Surgically resected materials from 214 patients were evaluated by histological observations. Seventy-nine patients (36.9%) with an intraductal carcinoma component infrequently developed large tumors and infrequently showed deep invasion and venous, lymphatic and perineural involvement in the main tumor nodule. An intraductal carcinoma component was inversely correlated with advanced clinical stage, and was shown to be a significantly favorable prognostic factor by both univariate and multivariate analyses. Proximal (hepatic) side bile duct resection margin status was categorized into negative for tumor cells, positive with only an intraductal carcinoma component [R1 (is)], and positive with a subepithelial invasive component (R1). Forty-five patients (21.0%) with an R1 resection margin had a poorer prognosis than 148 patients (69.2%) with a negative resection margin, whereas 21 patients (9.8%) with an R1 (is) resection margin did not. In patients with an R1 resection margin, the risk of anastomotic recurrence was higher, and the period until anastomotic recurrence was shorter, than in patients with an R1 (is) resection margin. Surgeons should not be persistent in trying to achieve a negative surgical margin when the intraoperative frozen section diagnosis is R1 (is), and can choose a safe surgical procedure to avoid postoperative complications. (*Cancer Sci* 2009; 100: 62–70)

Biliary tract carcinoma still has a poor prognosis, and most cases are at an advanced stage when patients present with symptoms. Previous studies of extrahepatic bile duct carcinoma and hilar cholangiocarcinoma have indicated that surgical resection is the only curative treatment for affected patients.[1–10] Biliary tract carcinoma is remarkable because of its tendency for superficial extension by wide intraductal carcinoma.[11–14] However, it is difficult to accurately estimate the extent of the intraductal carcinoma component in the biliary tract on the basis of preoperative imaging studies.[13,15–18] It is feasible that intraoperative histological diagnosis using frozen sections may detect tumor involvement at the bile duct resection margin. Surgeons are required to make an immediate decision about the resection area based on intraoperative frozen section diagnosis. However, to our knowledge, no previous study has examined the clinicopathological significance and prognostic impact of an intraductal carcinoma component with reference to bile duct resection margin status in patients with biliary tract carcinoma.

In this retrospective study, the presence or absence of an intraductal carcinoma component and bile duct resection margin status were evaluated by histological observations of all surgically resected materials from 214 patients with biliary tract carcinoma who underwent radical surgery with curative intent. In order to provide a yardstick for surgeons who depend on the results of frozen section diagnosis during surgery, we examined the correlation between an intraductal carcinoma component and bile duct resection margin status on the one hand, and clinicopathological parameters on the other, and also the prognostic impact of an intraductal carcinoma component and bile duct resection margin status.

Materials and Methods

Patients and specimens. The study included 214 patients with biliary tract carcinoma who underwent radical surgery with curative intent at the National Cancer Center Hospital, Tokyo, Japan, between May 1965 and December 2003. Patients who died in hospital or within 100 days after surgery, and patients who underwent biopsy or palliative surgery, were not included. The included patients comprised 150 men and 64 women, ranging in age from 33 to 83 (mean 63.4) years.

The main tumor nodule was located in the lower, middle and upper thirds of the extrahepatic bile duct, the entire extrahepatic bile duct, the hilar bile duct, and intrahepatic bile duct adjacent to the hilar area in 27, 38, 14, 5, 77, and 53 patients, respectively. Patients with carcinoma of the peripheral intrahepatic bile duct were excluded. Pancreatoduodectomy (PD), extrahepatic bile duct resection (EHBD), hepatic resection with extrahepatic bile duct resection (HR+EHBD), hepatic resection (HR) and combined hepatectomy and pancreatoduodectomy (HPD) were performed in 47, 19, 124, 16 and 8 patients, respectively. The formalin-fixed surgically resected specimens were cut into slices at intervals of 0.5–0.7 cm, and all the sections were embedded in paraffin and routinely processed for microscopical examination. All tumors were classified according to the pathological tumor-node-metastasis (TNM) classification.[19] Intrahepatic bile duct carcinomas adjacent to the hilar area, for which TNM criteria have never been established, were classified according to the TNM classification for extrahepatic bile duct carcinoma. This study was approved by the Ethical Committee of the National Cancer Center, Tokyo.

Evaluation of an intraductal carcinoma component and bile duct resection margin status. The intraductal carcinoma component was defined as carcinoma within the bile duct and its small branch outside the main tumor nodule consisting of a subepithelial invasive component (Fig. 1). For cases in which intraoperative frozen section diagnosis of the ductal stump had been performed, the proximal (hepatic) side bile duct resection margin status was histologically assessed by review of the frozen section and its re-fixed permanent section with reference

[5]To whom correspondence should be addressed. E-mail: ykanai@ncc.go.jp

doi: 10.1111/j.1349-7006.2008.01009.x

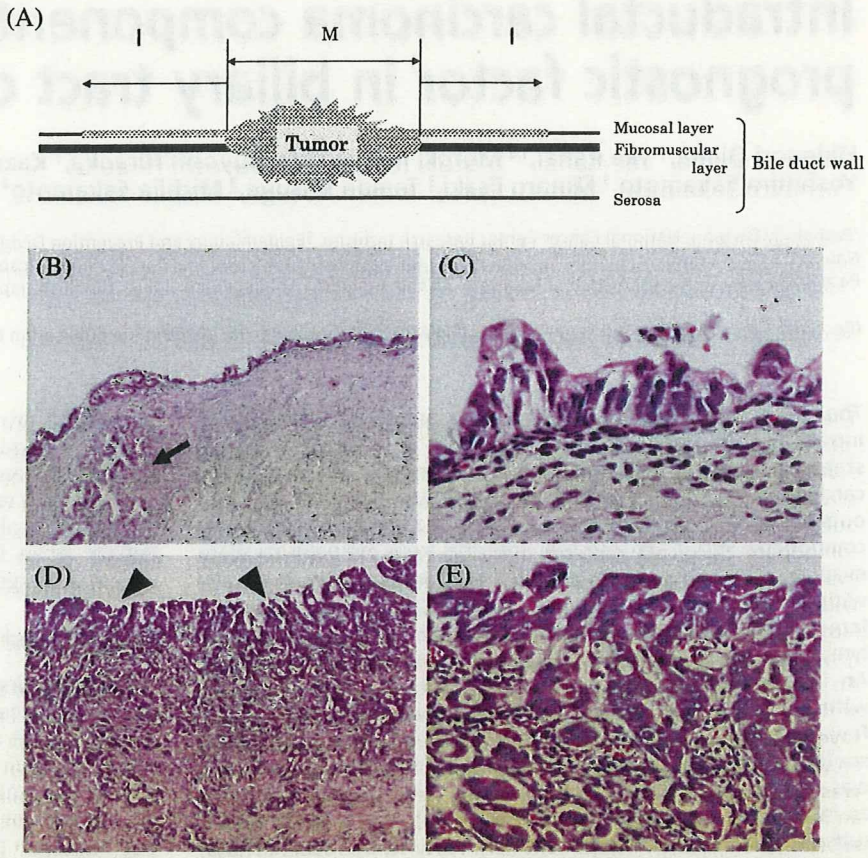

Fig. 1. Definition of an intraductal carcinoma component (I). (A) I is defined as intraductal carcinoma in the bile duct and its small branch outside the main tumor nodule (M) consisting of a submucosal invasive component. (B and C) Microscopic view of an example of I in the bile duct and its small branch (arrow). Hematoxylin and eosin (H&E) stain, original magnification ×40 (B) and ×400 (C). (D and E) Microscopic view of an example of M. Carcinoma *in situ* inside M (arrow heads) is not considered as I in this study. H&E stain, original magnification ×40 (D) and ×200 (E).

to the extent of the tumor in formalin-fixed surgically resected specimens. For cases in which intraoperative frozen section diagnosis of the ductal stump had not been performed, proximal side bile ductal resection margin status was histologically assessed by review of the formalin-fixed surgically resected specimens.

Follow-up and assessment of anastomotic recurrence at the bile duct resection margin. All 214 patients were followed for more than 100 days, and the mean duration of follow-up was 1215 days. Follow-up examination was performed using computed tomography, abdominal ultrasonography, and measurement of the serum carcinoembryonic antigen (CEA) and carbohydrate antigen 19-9 (CA19-9) levels every 3–6 months by surgeons. Anastomotic recurrence at the proximal side of the bile duct resection margin was diagnosed only in patients with a positive resection margin. In such patients, when a mass lesion was detected after dilatation of the bile duct in the residual liver because of obstruction of the anastomosis site, using radiological evaluation including computed tomography and ultrasonography, surgeons considered that the patient had anastomotic recurrence (not local recurrence in which perineural invasion around the hepatic artery and/or involved regional nodes first formed a mass lesion). Causes of death were determined from the medical records.

Statistical analyses. Correlations between presence or absence of an intraductal carcinoma component and bile duct resection margin status on the one hand and clinicopathological parameters on the other were analyzed using chi-squared test.

Person-days of follow-up were calculated from the date of surgical resection until date of death or end of the study period (March 8, 2005), whichever occurred first. The crude rate of all-cause deaths was calculated by dividing the number of deaths by the number of person-days. Similarly, person-days of follow-up were calculated from the date of surgical resection until date of death, date of diagnosis of anastomotic recurrence, or end of the study period (March 8, 2005), whichever occurred first. The crude rate of recurrence at the proximal side bile duct resection margin was calculated by dividing the number of cases with recurrence by the number of person-days. Survival curves were constructed using the Kaplan–Meier method, and differences in survival were evaluated using the log-rank test. The Cox proportional hazards model was used to estimate hazard ratio (HR) and 95% confidence interval (CI) of death or anastomotic recurrence by clinicopathologic factors using the SAS program (PROC PHREG) (SAS Institute Inc., Cary NC, US). All tests were two-sided and differences at $P < 0.05$ were considered statistically significant.

Results

Univariate analysis of correlation between an intraductal carcinoma component and clinicopathological parameters. An intraductal carcinoma component was positive in 79 (36.9%) of the 214 examined patients. Correlations between an intraductal carcinoma component and clinicopathological parameters were examined using univariate analysis (Table 1). Location of the main tumor nodule ($P = 0.007$), and histologic type ($P < 0.0001$) were significantly correlated with an intraductal carcinoma component (Table 1). Tumor size ($P = 0.01$), depth of invasion ($P < 0.0001$), venous involvement ($P < 0.0001$), lymphatic involvement ($P = 0.0006$), perineural involvement ($P < 0.0001$), the pathological assessment of the primary tumor (pT) ($P < 0.0001$), and pathological TNM stage ($P < 0.0001$) were each inversely correlated with presence of an intraductal carcinoma component: patients with an intraductal carcinoma component infrequently developed large tumors, infrequently showed deep invasion into the bile duct wall and venous, lymphatic and perineural involvement in the main tumor nodule, and were infrequently at an advanced stage when diagnosed (Table 1).

Table 1. Correlation between an intraductal carcinoma component and clinicopathological parameters in patients with biliary tract carcinoma

	No. of cases		*P* for difference*
	Intraductal carcinoma component		
	Negative ($n = 135$)	Positive ($n = 79$)	
Age (years)			0.01
<65	73	29	
≥65	62	50	
Sex			0.85
Male	94	56	
Female	41	23	
Location of the main tumor nodule			0.007
Lower third of extrahepatic bile duct	15	12	
Middle third of extrahepatic bile duct	17	21	
Upper third of extrahepatic bile duct	6	8	
Entire extrahepatic bile duct	2	3	
Hilar bile duct	54	23	
Intrahepatic bile duct	41	12	
Histologic type			<0.0001
Adenocarcinoma	129	55	
Papillary adenocarcinoma	1	21	
Others	5	3	
Tumor size (cm)			0.13
<3	54	40	
≥3	81	39	
Differentiation of adenocarcinoma			0.50
Well	34	18	
Moderate	80	29	
Poor	15	8	
Depth of invasion			<0.0001
Carcinoma *in situ* or invasion to fibromuscular layer	1	16	
Invasion into subserosa or beyond bile duct wall	134	63	
Venous involvement			<0.0001
Absent	6	19	
Present	129	60	
Lymphatic involvement			0.0006
Absent	9	18	
Present	126	61	
Perineural involvement			<0.0001
Absent	10	24	
Present	125	55	
pT classification			<0.0001
pT1-2	11	40	
pT3-4	124	39	
pN classification			0.06
pN0	64	48	
pN1	71	31	
TNM stage			<0.0001
0, IA, IB	8	32	
IIA	53	14	
IIB	62	28	
III	12	5	

*Chi-squared test.

Univariate analysis of correlation between an intraductal carcinoma component or clinicopathological parameters on the one hand and prognosis of patients on the other. Overall survival rates after resection were 33.2% at 5 years and 22.9% at 10 years. Hazard ratio (HR) and 95% confidence interval (CI) of all-cause deaths by an intraductal carcinoma component and other clinicopathological parameters were examined using univariate analysis (Table 2). Patients with an intraductal carcinoma component showed a significantly more favorable prognosis than patients without such a component (Table 2).

Multivariate analysis of prognostic impact of an intraductal carcinoma component. When all 214 patients were examined by multivariate analysis adjusted for age, operation day, type of surgical resection, tumor size, histologic type and tumor differentiation, depth of invasion, venous involvement, lymphatic involvement, perineural involvement and TNM stage, patients with an intraductal carcinoma component showed a significantly more favorable prognosis than patients without such a component (Table 3). When only the 117 patients who underwent complete resection (proximal side bile duct resection margin for all

doi: 10.1111/j.1349-7006.2008.01009.x

Table 2. Crude hazard ratio (HR) and 95% confidence interval (CI) of all-cause deaths by an intraductal carcinoma component and clinicopathological parameters

	No. of deaths	Person-days	Crude death rate†	Crude HR	95% CI	*P* for trend
Intraductal carcinoma component						
Negative	96	136 804	70.2	1.00		
Positive	35	123 209	28.4	0.39	0.27, 0.58	
Age (years)						
<65	58	137 562	42.2	1.00		
≥65	73	122 451	59.6	1.33	0.94, 1.87	
Sex						
Male	94	179745	52.3	1.00		
Female	37	80 268	46.1	0.84	0.57, 1.23	
Location of the main tumor nodule						
Lower third of extrahepatic bile duct	17	43 899	38.7	1.00		
Middle third of extrahepatic bile duct	23	43 696	52.6	1.04	0.56, 1.96	
Upper third of extrahepatic bile duct	10	18 228	54.9	1.17	0.54, 2.56	
Entire of extrahepatic bile duct	3	4837	62.0	1.07	0.31, 3.67	
Hilar bile duct	46	87 502	52.6	1.09	0.63, 1.91	
Intrahepatic bile duct	32	61 851	51.7	1.14	0.63, 2.06	
Histologic type						
Adenocarcinoma	123	211 330	58.2	1.00		
Papillary adenocarcinoma	5	37 000	13.5	0.25	0.10, 0.62	
Others	3	11 683	25.7	0.51	0.16, 1.61	
Tumor size (cm)						
<3	46	134 392	34.2	1.00		
≥3	85	125 621	67.7	1.82	1.27, 2.61	
Differentiation of adenocarcinoma						
Well	36	70 278	51.2	1.00		
Moderately	67	126 210	53.1	1.13	0.75, 1.69	
Poorly	20	14 842	134.8	2.56	1.47, 4.44	
Depth of invasion						
Carcinoma *in situ* or invasion to fibromuscular layer	3	37 435	8.0	1.00		
Invasion into subserosa or beyond bile duct wall	128	222 578	57.5	6.44	2.04, 20.3	
Venous involvement						
Absent	6	63 305	9.5	1.00		
Present	125	196 708	63.5	5.80	2.54, 13.3	
Lymphatic involvement						
Absent	9	76 294	11.8	1.00		
Present	122	183 719	66.4	4.67	2.25, 9.67	
Perineural involvement						
Absent	11	72 565	15.2	1.00		
Present	120	187 448	64.0	3.67	1.95, 6.89	
pT classification						
pT1-2	23	89 367	25.7	1.00		
pT3-4	108	170 646	63.3	2.32	1.47, 3.66	
pN classification						
pN0	57	176 738	32.3	1.00		
pN1	74	83 275	88.9	2.56	1.80, 3.65	
TNM stage						
0,IA,IB	15	77 359	19.4	1.00		<0.01
IIA	39	91 428	42.7	2.26	1.24, 4.12	
IIB	65	75 858	85.7	4.21	2.37, 7.46	
III	12	15 368	78.1	3.80	1.77, 8.15	

†per 100 000 person-days.

patients, distal [duodenal] side bile duct resection margin for patients who underwent HR + EHBR, resected margin of the pancreas for patients who underwent PD were all negative) were examined in order to eliminate the effect of surgical curability, an intraductal carcinoma component was still a favorable prognostic factor (Table 3).

Correlation between an intraductal carcinoma component and bile duct resection margin status. Although an intraductal carcinoma component has been proven to be a favorable prognostic factor, it is feasible that patients with such components frequently have tumor involvement at the bile duct resection margin. Therefore, the correlation between an intraductal carcinoma component and proximal side bile duct resection margin status (negative or positive) was examined statistically (Table 4). An intraductal carcinoma component was found to be correlated with bile duct resection margin status: patients with an intraductal carcinoma component more frequently had a positive resection margin than patients without such a component ($P = 0.0192$, Table 4). In